

Behavior of HV Cable at Short Circuit

Alex Pokryvailo

Spellman High Voltage Electronics Corporation
475 Wireless Blvd
Hauppauge NY 11788, USA

ABSTRACT

In our previous work, we analyzed an unusual behavior of an HV cable at short circuit when the shield at the power supply side was grounded, and at the load side it was floating. It was shown that the transmission line model is no longer applicable. It was also shown that the cable insulation is overstressed at the load side. Staying within a convenient simplicity of a two wire line approximation it was still possible analyzing salient phenomena of the load breakdown in unterminated shield connection. However, the period of oscillations T for this case was almost four times greater than could be expected from the cable electrical length! We did not address this discrepancy previously; to the best of our knowledge, it was not described in literature. Here, we analyze the reasons for the dramatic increase of T . Again, main tools are lumped circuit simulation and experiments on low-voltage increase model lines. The first suggests that since the currents in the central conductor and the shield flow in the same direction, the resulting circuit inductance is much greater than that in a conventional line discharge. Such inductances have been estimated. Experiments showed that the cable (coiled or spread) and ground layouts have also large influence on T . Experiments with an HV cable at a voltage up to 40 kV increased confidence in the simulation and low-voltage physical modeling results. Overall, simulation and experimental results are in fair agreement.

Index Terms - Unterminated shield connection, high voltage cable, breakdown, transmission line, loop inductance, PSpice

1 INTRODUCTION

THE previous paper [1], before the present one was envisioned, dealt mostly with the practical problems of load shorts in the form of a spark, followed by a “permanent” short in the form of an arc. In particular, it analyzed an unusual behavior of a high voltage (HV) cable of a HV power supply (PS) at short circuit, when the shield at the PS side was grounded, and at the load side it was floating. We called it “unterminated shield connection”, or UTSC. Such connection is convenient and thus ubiquitous in number of applications. To name a few, they are electrostatic precipitation (mostly low-power installations), ion implantation, and HV testing and general laboratory practice. We are unaware of UTSC use in power transmission and distribution systems. It was shown, both experimentally and theoretically, that the cable shield voltage at the distal (load) end oscillates with amplitude approaching that of the PS voltage. Thus, the cable insulation is overstressed at the load side. It was also shown that the transmission line (TL) model was no longer applicable, because the currents in the central conductor and the shield are not equal and do not necessarily flow in opposite directions. Actually, in UTSC we deal with a *three*-conductor

TL, the third conductor being ground. This conductor may be formed by both intentional ground wire and unintentional, parasitic wiring, and thus a concept of a multiwire TL needs to be invoked. However, staying within a convenient simplicity of a two-wire line approximation by lumped ladder circuits it was still possible to analyze salient phenomena of the load breakdown in UTSC. PSpice simulations [1] did yield waveforms *qualitatively* similar to their experimental counterparts. However, the period of oscillations T in an UTSC was almost four times greater than could be expected from the cable electrical length! This discrepancy was not addressed in [1], and, to the best of our knowledge, is not described in literature. The rest of this paper strives to explain the observed mismatch.

2 EXPERIMENTAL

We start with experimental investigation since it provides vivid means to expose the essence of the problem. First, the experiments on a model TL at low voltage (LV) are presented. They are followed by HV tests with a real HV cable.

2.1 LOW VOLTAGE TESTS

The LV test setup is depicted in Figure 1. Basically, it reproduces that described in [1], with some modifications

as required for this particular investigation. Two sections of about 5.5-m-long RG-58 cables (total length is approximately 11 m; electrical length is about 58 ns) joined with a BNC Tee were charged from a DC PS up to 60 V through a high-value limiting resistor. The latter imitates arc-limiting means of a PS and isolates PS from the cable during cable discharge. The cable was either coiled or spread in line or arranged in some other manner. An aluminum grounded plate could be placed under the coiled cable. This case is actually drafted in Figure 1, where “solid ground” refers to the aforementioned plate. Alternatively, the plate could be removed, in which case the grounds of the PS and the gate driver (function generator Tabor 8020) were not connected directly through a low-impedance path, but through the building wiring. The layout of the latter was unknown. The purpose of different cable arrangements was determining their influence on the resulting oscillations.

Note that the difference in the cable physical layout changes the capacitance of the cable shield to both ground and between the adjacent parts of the shield itself. Likewise, the inductance of cable conductors and ground wiring that form the current loop of this multi-wire line also depends on the layout.

The cable was discharged to ground in a repetitive mode using a fast MOSFET IRFD110 (switching time was <5 ns—see Figure 8 in [1]). The cable voltages were monitored by a TDS3034 scope with P6139A probes. Several control measurements were performed with differential probes P5200 to exclude possible influence of ground clips. The voltages were typically monitored in two points: at TL start and its distal end.

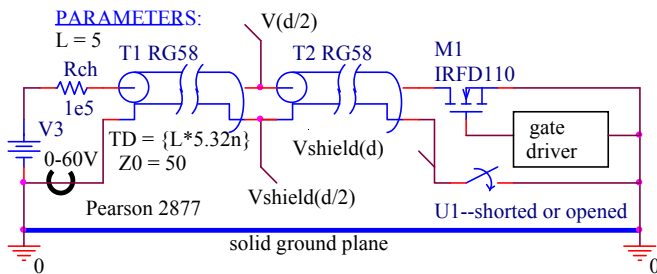


Figure 1. Experimentation scheme. Ground plane is removable. Switch U1 is open in UTSC.

The central conductor and the shield potentials at these points are denoted as $v(0)$, $v(d)$, $v_{\text{shield}}(0)$ and $v_{\text{shield}}(d)$, respectively. In addition, the current at the shield proximal end was monitored with a Pearson current transformer, model 2877 (risetime 2 ns). The discharge current could be also measured at other points, e.g., at TL end, as shown in Figure 1.

A reference experiment, as before, was shorting the line with shield connected to ground at distal end. The expected quasi-rectangular pulses and almost full reversal of voltage and current at proximal and distal ends, respectively, were observed (in this work, the waveforms were a replica of Figure 9 of [1]; they are not reproduced here). The oscillation

period corresponded to the electrical length and was $T \approx 240$ ns.

The waveforms shown with the Tektronix Wavestar software typically include the voltages on the central conductor and the shield, and the shield current, as denoted above. Horizontal and vertical scales are given, per division, in the inset captions on the screen shot bottom, and the period of oscillations is measured between the vertical cursors. It is indicated in the upper right part of the screen as dX.

With the purpose of investigating the influence of the cable and return ground conductors layout on the period of oscillations, the cable was arranged in several ways. The experimental results for the five following cases, all with UTSC, are briefly summarized below.

1. The cable was stretched in an approximately straight line. PS and gate driver were on the different TL ends, i.e., about 10 m apart. Only shield current at proximal end (it is CH2 in all screens) was measured to determine $T=1.07 \mu\text{s}$ Figure 2 which is greater than in similar waveforms fig. 10 of [1], where the cable was coiled and placed on a ground plate.
2. The cable formed approximately 5-m-long, 1-m-wide loop. Ground plane was removed. Figure 3 shows the shield current at proximal end and the shield voltage at distal end (CH3). Period of oscillations was $T=0.844 \mu\text{s}$.
3. Cable was loosely coiled in a circular loop having 15 turns (approximately 0.2 m diameter) Figure 4. $T=1.71 \mu\text{s}$.
4. Cable was coiled as above, except the coiled cable was placed on a grounded square aluminum plate with a 0.4-m-side. This experiment was similar to its counterpart in [1] where all bench was covered by a grounded metal plate. Period of oscillations decreased to $T=0.87 \mu\text{s}$. See Figure 5, in which a trace of the voltage on the central conductor, CH1, at the proximal end is added.
5. Cable was coiled as above and clamped by a U100/57/25 core (3C90 material). Period of oscillations sharply increased: $T=7.47 \mu\text{s}$. See Figure 6.

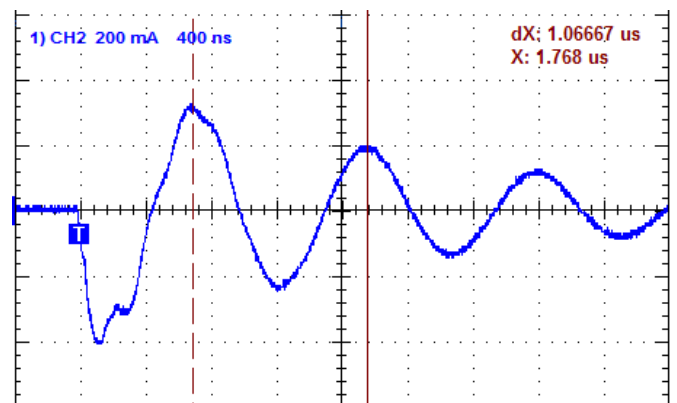


Figure 2. Shield current at proximal end. Vertical – 200 mA/div, horizontal – 400 ns/div (see scale in waveform note). Cable was spread in line. PS and gate driver were on the different TL ends, approximately 10m apart. No ground plate.

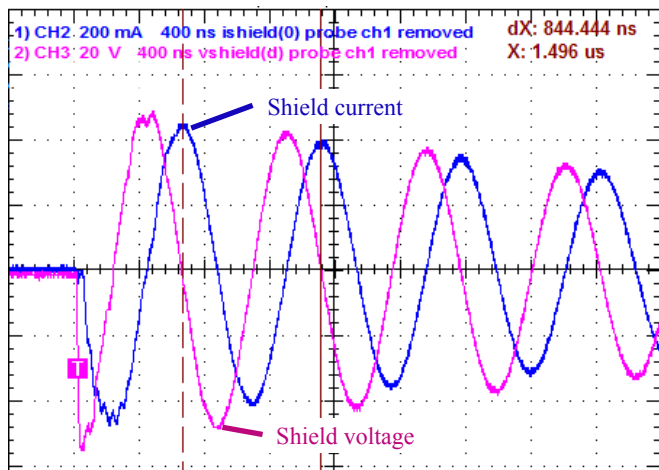


Figure 3. Shield current at proximal end (CH2, 200 mA/div) and shield voltage at distal end (CH3, 20 V/div). Cable formed approximately 5-m-long, 1-m-wide loop. No ground plate.

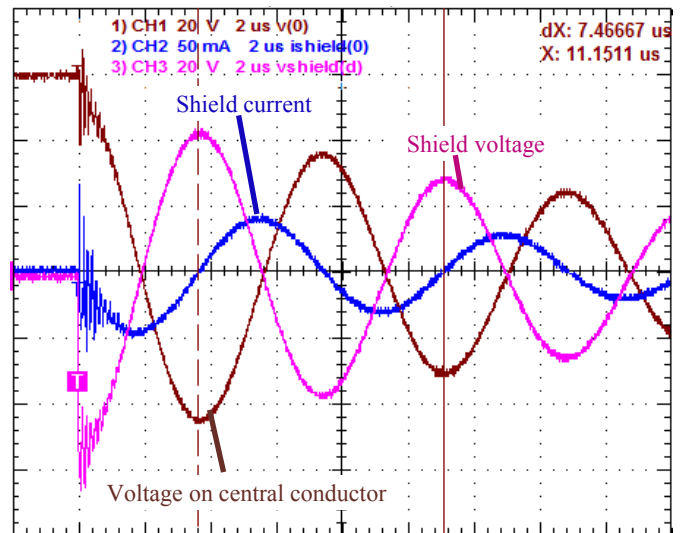


Figure 6. Same as in Figure 4, except the coil was clamped by a U100/57/25 core (3C90 material). No ground plate.

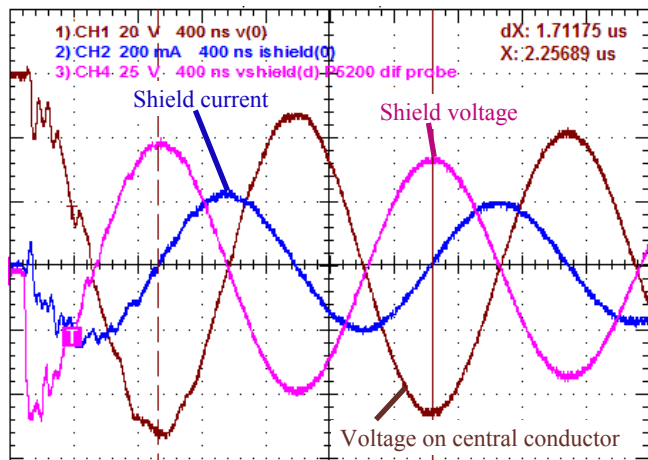


Figure 4. Voltage on central conductor at proximal end CH1 – 20 V/div), shield current at proximal end (CH2, 200 mA/div) and shield voltage at distal end (CH4, 25 V/div). Cable was loosely coiled in a circular loop having 15 turns (approximately 0.2-m diameter). No ground plate.

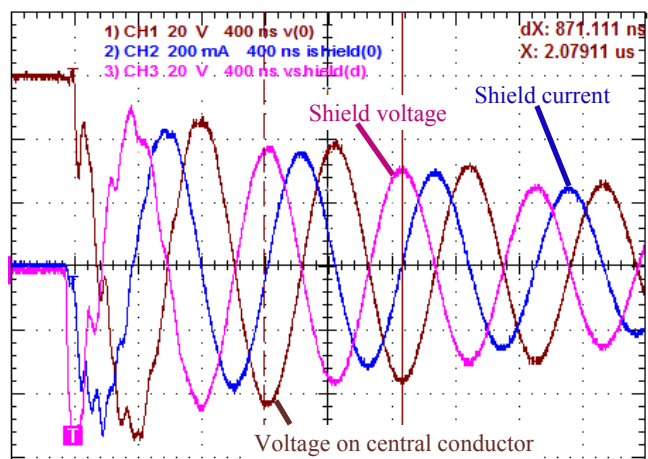


Figure 5. Same as in Figure 4, except the coiled cable was placed on grounded aluminum plate.

All these and similar experiments evidenced that the oscillation frequency was much larger than that expected from the cable electrical length. It was determined mostly by the cable arrangement and had little to do with speed of propagation of electromagnetic wave in the cable, contrary to a usual short between the central conductor and the shield. In particular, in any of the above arrangements with the shield distal end grounded, the oscillations were the same, matching the cable electrical length ($T \approx 240$ ns).

2.2 HV TESTS

The HV setup was not different from its LV counterpart Figure 1 schematic-wise. A Spellman single-phase input SL130kV positive polarity HV PS charged a 12.5-m HV cable (Dielectric Sciences 150 kV polyethylene cable model 2121). On the PS side, the shield was connected to the grounded chassis via a coaxial bushing, and on the distal (load) end the shield was stripped on the length of 0.4 m forming what was termed a “flush cut termination” in [2]. In view of a coaxial connection at the PS side, the shield current there was not measured. At the distal end, the shield was left floating, and its potential was monitored by a Tektronix P6015A probe. The cable was coiled in 7 turns with coil diameter of approximately 0.37 m (mean diameter) leaving about 2 m of uncoiled length to allow safe connections inside the HV cage (the PS stayed outside of the cage). The closing switch was formed by two large smooth toroidal electrodes in ambient air, so no corona preceded the breakdown. Maximum voltage was limited to about 40 kV, mostly by the P6015A probe. The LV electrode was connected to the cage ground by a 1-m wire on which a Pearson 2878 current monitor (4 ns risetime) was threaded. Besides the line cord ground wire, the PS chassis was connected to the cage ground by a 2-m wire. Thus, a star grounding scheme with well-defined connections was employed, although we did not take special care to decrease the layout inductances.

Typical waveforms of the short circuit current and shield voltage are shown in Figure 7. The period of oscillations is here $T=0.9\ \mu\text{s}$, measured after the first half-wave of the shield voltage. (Note almost rectangular shape of this first half-wave and sharp decrease of the rate of rise after zero-crossing.)

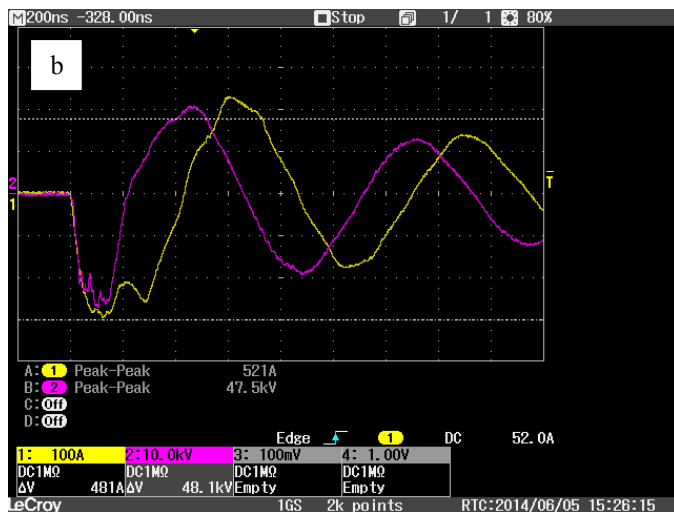
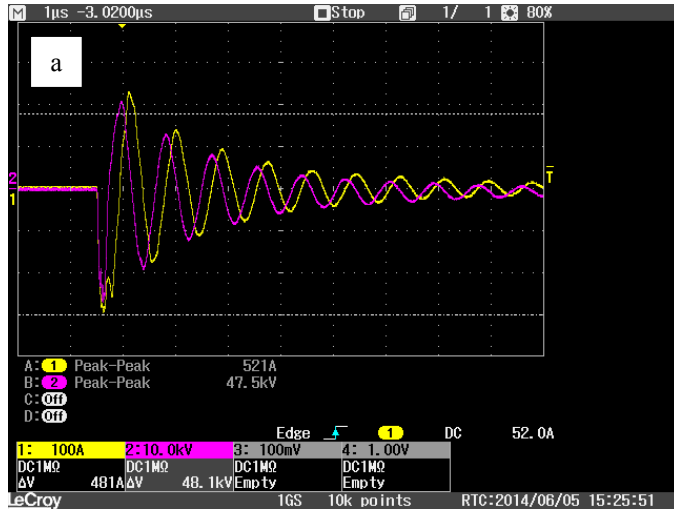


Figure 7. Short circuit current (ch1, 100 A/div) and shield voltage (ch2, 10 kV/div). Breakdown voltage 40 kV. Horizontal a – 1 μs/div, b – 200 ns/div.

Although the HV tests at a relatively low voltage did not provide essentially new information as compared to their LV counterparts (which was expected from the linear nature of the described systems), we feel obliged to report the results for greater confidence. At full voltage, breakdowns with long cables may be detrimental [1], which certainly was not intent of this investigation.

In the next section, we make theoretical estimates for the experimental scenarios. These estimates deal mainly with the

influence of the cable arrangement on the loop inductance, as depicted above in the selected five cases of LV experiments.

3 THEORETICAL

It was already noted in [1] that a basic assumption in deriving telegraphic equations for a *two-conductor* transmission line is that both conductors carry only differential currents that are equal to each other in every line cross-section [3]-[5]. If the shield at distal end is lifted off-ground, the shield conduction current at this end is zero, but its counterpart in the central conductor reaches its maximum value as can be clearly seen from Figure 1 and experimental waveforms of the previous section. On the opposite, at the proximal end, the central (forward) conductor current is zero, and the shield current is at its maximum. Thus, considering just these observations, we may conclude that the classical two-wire TL model does not support the UTSC case.

In UTSC we deal with a *three-conductor line*, the third conductor being ground. (Whether this line behaves as a TL is another matter.)

We will continue using lumped circuit modeling, one of the reasons being that it allows PSpice modeling. We reiterate that we cannot use traditional equivalent circuit (EC) used for deriving telegraph equations [5] by the above formulated reasons. Rather, we distribute the line inductance between the forward and return conductors, so that the total cell inductance remains the same. Figure 8 is an example of such a model having 10 cells (for convenience: our LV test cable is about 10-m-long, so each cell represents 1/10 of this length). This model is more intricate than that used in [1]. It distinguishes between the inductance of the central conductor, L_{c_in} , and shield, L_{sh} . It also includes the ground conductor inductance L_g and capacitance to the shield C_{sh_g} . Capacitance $C_g=93.5\ \text{pF}$ is the RG58 cable capacitance per unit length (between the central conductor and the shield). The nature and value of all these parameters, except C_g , are not easy to determine in the case of UTSC.

A reduced EC is shown in Figure 9. Here the central conductor and shield inductances L_{in} are equal.

In our case, the currents in the central and in the shield conductors flow in the same direction, returning via ground conductor. Thus, both cable conductors can be approximated by a single wire that can be stretched, looped, coiled, etc. The inductance of such a wire is much larger than the inductance of a coaxial cable. It should be also made clear that, following from the current continuity principle, the ground wire current must equal the sum of the currents in the cable conductors. We note that usually a loop inductance concept is invoked, an assumption being that the current forms a closed loop. (In such a way, for instance, the inductance of a coaxial cable is calculated.) A solitary wire inductance is also a loop inductance, but the return conductor is infinitely remote.

Now we will examine quantitatively the cases presented in the Experimental Section.

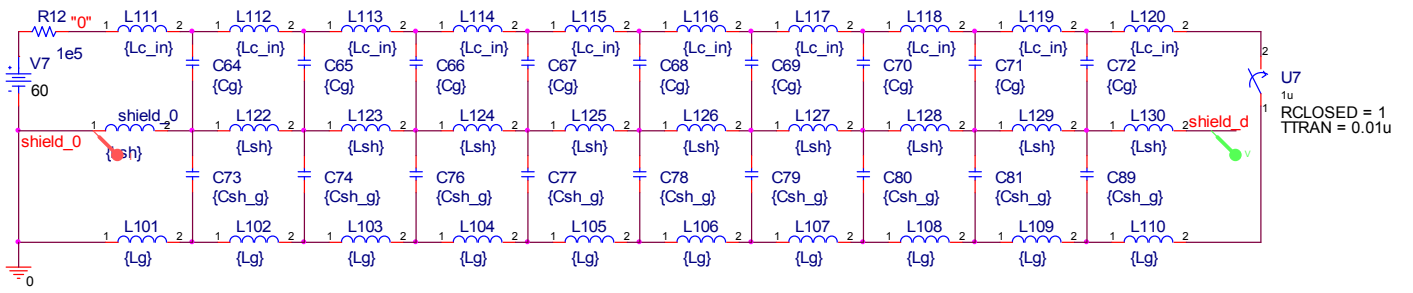
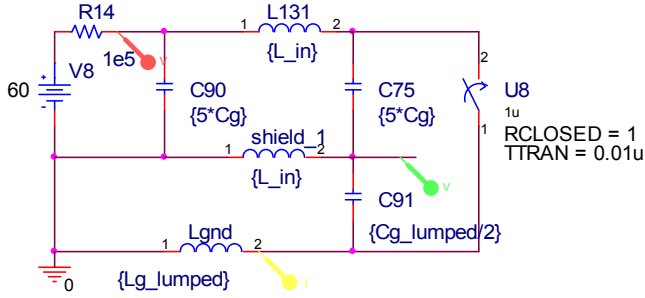


Figure 8. Cable equivalent circuit for UTSC.


 Figure 9. Reduced equivalent circuit. Note that total capacitance of C90 and C75 imitating the cable is $10 * C_g$.

Consider the cable stretched in a straight line. Assuming it to be a solid round conductor, we can estimate its inductance as [6]

$$L_{rw} = \frac{\mu_0}{2\pi} l \left(\ln \frac{2l}{\rho} - \frac{3}{4} \right) \quad (1)$$

in a low frequency approximation, or

$$L_{rw} = \frac{\mu_0}{2\pi} l \left(\ln \frac{2l}{\rho} - 1 \right) \quad (2)$$

for very high frequency approximation. Here $l=10$ m is the length, and $\rho=0.0015$ m is the wire radius. With these values, $L_{rw}=17.5$ μ H and $L_{rw}=17$ μ H calculated by equations (1) and (2), respectively. If there is a return conductor in a form of the same straight wire spaced by 10 m, the inductance is doubled. It is difficult to determine where the return conductor in our experiments is (and in real-life applications!) unless there is a visible path, e.g., in a form of a ground plane.

The estimate (1) is for a single conductor, so in the ECs Figure 8, Figure 9 we must account for splitting the inductance by doubling the values, since the inductances are connected in parallel. Thus, we adopt $L_{c_in}=L_{sh}=2*17.5/10=3.5$ μ H in Figure 8, and $L_{in}=35$ μ H in Figure 9. With L_g , C_{sh_g} and L_{g_lumped} and C_{g_lumped} tending to zero, we obtain the waveforms shown in Figure 10. The top and bottom plots are for Figure 9, Figure 8, respectively. The periods of oscillations for them are $T=0.829$ μ s and $T=0.924$ μ s. This is not far from the experimental $T=1.067$ μ s (see Figure 2). Better match to the experiment is with $L_g=0.1L_{g_lumped}=1$ μ H ($T=1.01$ μ s and $T=1.08$ μ s), which probably represents the ground conductor

inductance more accurately. Note that just calculating the resonant frequency in the LC loop formed by the cable capacitance and L_{rw} gives $T=0.802$ μ s.

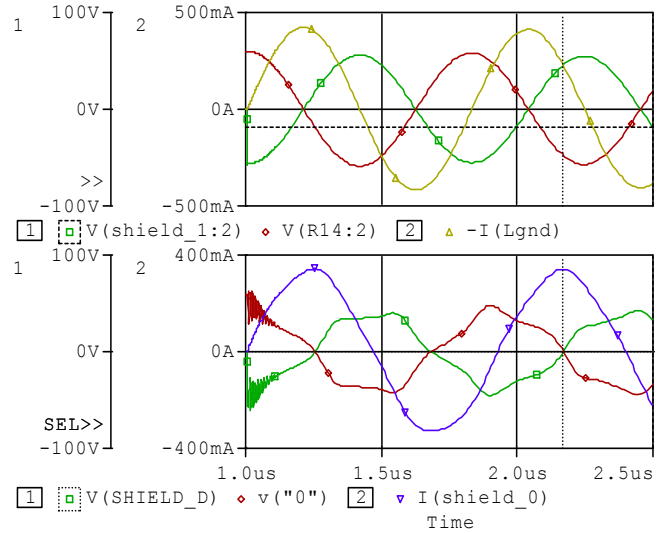


Figure 10. Simulation of circuit Figure 8 and Figure 9 (bottom and top plots, respectively).

For the cable spread in a 5-m-long, 1-m-wide loop, we calculate the inductance using a formula for a two-wire TL [6]:

$$L_{long_loop} = \frac{\mu_0}{\pi} l \left(\ln \frac{d}{\rho} - \frac{\rho^2}{d^2} - \frac{3\rho^4}{2d^4} \right) \quad (3)$$

For $l=5$ m, $L_{long_loop}=13$ μ H. Simulation Figure 8 with vanishing L_g , C_{sh_g} values yields $T=0.8$ μ s, which is close to its experimental counterpart $T=0.844$ μ s in Figure 3.

The coiled cable inductance can be estimated by a formula derived for a round loop with diameter d having a round cross-section of radius a [6]:

$$L_{round_loop} = \frac{\mu_0}{2} N^2 d \left(\ln \frac{4d}{a} - \frac{7}{4} + \frac{a^2}{2d^2} \ln \left(\frac{4d}{a} + \frac{1}{3} \right) \right), \quad (4)$$

where N is number of turns in the coil.

Calculating for the coiled cable Figure 4 (the inductance of a 15 turn, 0.2-m-diameter coil with $a=1$ cm is about 75 μ H) yields $T = 2\pi\sqrt{7.457 \times 10^{-5} \times 93 \times 10^{-11}} = 1.655$ μ s

versus the experimental $T=1.71\ \mu\text{s}$. With the coiled cable placed on an aluminum plate, T becomes smaller because the induced currents decrease the inductance Figure 5. It is also obvious why the coiled cable clamped by a ferromagnetic core has much lower resonant frequency, as clearly seen in Figure 6.

Finally, we estimate the oscillation period of the HV cable arranged as described in Section 2.2: $d=0.37\ \text{m}$, $N=7$, $a=0.05\ \text{m}$ (7 turns loosely bundled). With the cable capacitance of 1.09 nF (this is a measured value), neglecting straight sections, we obtain $T=904.5\ \text{ns}$ (compare to Figure 7).

All these examples show that the oscillations in UTSC have little to do with wave propagation in the cable (of course, the first hundred or so of nanoseconds, in our case of a 10-m-long cable, are the wave processes); they are determined by the lumped parameters of the system. Notably, the reduced EC yields smooth sine waveforms that are close in shape to their experimental counterparts.

4 CONCLUSIONS

It has been shown that in UTSC the currents in both the central conductor and the shield flow unidirectionally. Therefore, the loop inductance of the cable during short circuit of the potential conductor, including the ground return, is largely determined by the cable and ground wires physical layout. This inductance is much larger than that of a coaxial cable. Accordingly, the oscillations in a cable having unterminated shield occur at a much lower frequency than wave reflections in a conventionally terminated cable at load shorts. These oscillations are determined largely by the lumped parameters of the system.

REFERENCES

- [1] A. Pokryvailo and C. Scapellati, "Behavior of HV Cable of Power Supply at Short Circuit and Related Phenomena", IEEE Trans. Dielectr. Electr. Insul., Vol. 20, No. 1, pp. 28-33, 2013.
- [2] A. Pokryvailo, C. Carp and C. Scapellati, "Comparative Testing of Simple Terminations of High Voltage Cables", IEEE Electr. Insul. Mag., Vol. 26, No. 1, pp. 7-17, 2010.
- [3] G. Miano and A. Maffucci, *Transmission Lines and Lumped Circuits*, Academic Press, NY, 503p, 2001.
- [4] C. R. Paul, *Analysis of Multiconductor Transmission Lines*, Wiley, NY, 821p, 2008.
- [5] K. A. Krug, *Foundations of Electrotechnics*, 6th ed., in two volumes, Gosenergoizdat, Moscow, 1946 (in Russian).
- [6] P. L. Kalantarov and L. A. Zeitlin, "Inductance Calculation", 3rd Ed., Leningrad, EnergoAtomizdat, 1986 (in Russian), 488pp. See also F.W. Grover, "Inductance Calculations", Dover, NY, 1946.



Alex Pokryvailo (M'05–SM'07) was born in Vyborg, Russia. He received the M.Sc. and Ph.D. degrees in electrical engineering from the Leningrad Polytechnic Institute in 1975 and 1987, respectively. Formerly with Soreq NRC, Israel, now he is with Spellman High Voltage Electronics Corp., serving as Director of Research. His current and recent experience relates to design of HV high-power switch-mode power supplies, Pulsed Power, with emphasis on high-current opening and closing switches and magnetic design, fast diagnostics, and corona discharges. Previously, he studied switching arcs, designed SF6-insulated switchgear, made research in the area of interaction of flames with electromagnetic fields, etc. He has published over 120 papers, two textbooks (in Hebrew), and more than 20 patents pertaining to HV technology.